Laser and Particle Beams (2005), *23*, 137–142. Printed in the USA.

DOI: 10.1017/S0263034605050226

Compression of a cylindrical hydrogen sample driven by an intense co-axial heavy ion beam

M. TEMPORAL,[1] J. J. LOPEZ CELA,[1] A. R. PIRIZ,[1] N. GRANDJOUAN,[2] N. A. TAHIR,[3] AND D. H. H. HOFFMANN[3,4]

[1]ETSII, Universidad de Castilla-La Mancha, Ciudad Real, Spain
[2]École Polytechnique–CNRS–CEA–Université Paris VI, Palaiseau, France
[3]Gesellschaft für Schwerionenforschung (GSI), Darmstadt, Darmstadt, Germany
[4]Institut für Kernphysik, Technische Universität, Darmstadt, Germany

(Received 30 November 2004; Accepted 10 December 2004)

Abstract

The compression of a cryogenic hydrogen cylindrical sample contained in a hollow gold target driven by an intense co-axial uranium beam has been studied. The ion distribution is assumed to be Gaussian in space and parabolic in time. The hydrodynamics of the target is analyzed by means of one- and two-dimensional numerical simulations. A parametric study is performed to achieve the maximum average hydrogen density and temperature as a function of the sample radius, total number of ions and spread of the spatial ion distribution. A window in the beam-target parameters for which hydrogen compression is higher than a factor of 10 and temperature is below 0.2 eV has been found by considering a single bunch that contains 2×10^{11} uranium ions delivered in 100 ns. In this range of high densities and low temperatures, it is expected that hydrogen may become metallic.

Keywords: Heavy ion beam; High density energy matter

1. INTRODUCTION

The study of matter under pressures of several Mbar and compressed to several times solid density is of great interest to different interdisciplinary sciences. Many studies were performed in relation to astrophysics phenomena (Remington *et al*., 1999) and inertial confinement fusion (Lindl, 1995). Theoretical and experimental works were also carried out during the past few decades to investigate equation of state properties of matter samples at extremely high pressures (Anisimov *et al*., 1984; Zeldovich & Raizer, 1967; More *et al*., 1988; Godwal *et al*., 2003). Hydrogen is one of the most interesting materials in this respect. As early as 1935 it was theoretically predicted that hydrogen at a pressure of 0.25 Mbar should experience a phase transition from an insulator to a metallic state (Wigner & Huntington, 1935). Modern estimates suggest that this phase transition should occur at a density around 1 g/cm^3, temperatures below a few thousand Kelvin and at pressures of the order of a few Mbar (Weir *et al*., 1996; Nellis *et al*., 1992).

Address correspondence and reprint requests to: M. Temporal, ETSII, Universidad de Castilla-La Mancha, 13071, Ciudad Real, Spain. E-mail: mauro.temporal@uclm.es

Shock waves generated by high power laser (Koenig *et al*., 1995; Nuckolls *et al*., 1972; Benuzzi *et al*., 1996; Cauble *et al*., 1997; Collins *et al*., 1998; Batani *et al*., 2003), X-rays (Cauble *et al*., 1993), gas-gun (Nellis *et al*., 1992), flyer-impact (Fabbro *et al*., 1986; Cottet *et al*., 1984; Obenschain *et al*., 1983), and nuclear explosions (Ragan 1980, 1984; Ragan *et al*., 1977) have been largely used to generate states of matter at Mbar pressures. The increased ion beam intensities provided by large heavy ion accelerators allow for considering heavy ions as a promising tool to generate and investigate matter at these high-density conditions and subjected to pressures of the order of Mbar.

Gesellschaft für Schwerionenforschung (GSI), Darmstadt, is a unique laboratory worldwide, it has a heavy ion synchrotron (SIS-18) with 18 Tm magnetic rigidity, which delivers intense heavy ion beams. Currently it delivers uranium ion beam with an intensity $N_U = 4 \times 10^9$ particles with an energy of 500 MeV/u and a pulse duration, τ of a few hundred ns. The optimum design of the SIS-18 will deliver a beam with $N = 2 \times 10^{11}$, $\tau = 50$ ns, and a particle energy of 200 MeV/u.

GSI is also constructing a new synchrotron ring SIS-100 (Henning, 2004) which will have a magnetic rigidity of 100

Tm and a circumference larger than 1 km. Design study has shown that this new facility will deliver a uranium beam with an intensity of 2×10^{12} particles per bunch. A wide range of particle energy will be available (400 MeV/u–2.7 GeV/u). Theoretical calculations have shown that using nonlinear bunch rotation one can achieve pulse duration of 20–90 ns for the above beam parameters (Tahir *et al.*, 2004). Possibility for availability of heavy ion beams with such high intensities has motivated several theoretical studies to design future experiments on equation of state of high-energy-density experiments using these beam parameters (Tahir *et al.*, 2000, 2001; Temporal *et al.*, 2003).

In the present paper, we present a target design of a new experiment that can be performed using the beam at the future SIS-100 facility. The target consists of a solid cylinder of frozen hydrogen enclosed in a shell of gold that is axially irradiated by an intense uranium ion beam. The target implosion is simulated using the one-dimensional (1D) hydrodynamic code MULTI (Ramis *et al.*, 1988) and the two-dimensional (2D) hydro-code CAVEAT (Addessio *et al.*, 1990). A compression of a factor 10 has been achieved in hydrogen while the temperature is below 0.2 eV considering a uranium beam delivering 2×10^{11} ions bunched in a $\tau = 100$ ns pulse length.

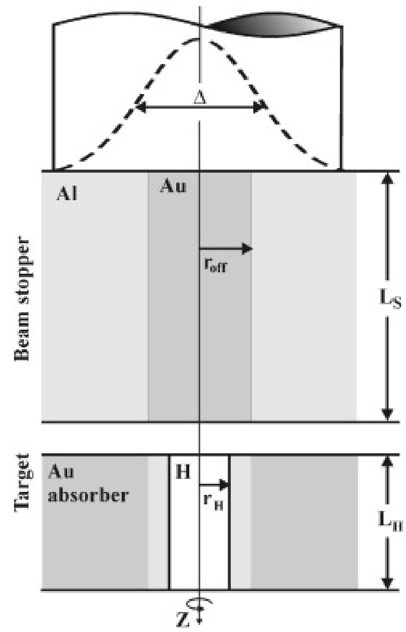

Fig. 1. Sketch of the simulated beam-target configuration. Cylindrical hydrogen sample with a beam stopper located between the incoming ion beam and the hydrogen sample. The graph it is not to scale.

2. BEAM TARGET INTERACTION

The success of inertial fusion energy, as well as high energy density physics experiments depend on the availability of sophisticated targets which match the conditions set by the intense ion or laser beam (Borisenko *et al.*, 2003). Here we consider a target that consists of a gold layer with a density $\rho_{Au} = 19.3$ g/cm^3 that encloses a cylindrical cryogenic hydrogen sample having a density $\rho_H = 0.0886$ g/cm^3, temperature $T_H = 10$ K, radius r_H, and target length L_H. An intense uranium ion bunch axially irradiates the target as schematically shown in Figure 1. The bunch delivers N_U uranium ions in a pulse which has a particle distribution that is Gaussian in space and parabolic in time while the pulse length, $\tau = 100$ ns.

The parabolic time dependence $f(t)$ of the ion beam is given by $f(t) = 6\,(t\tau - t^2)/\tau^2$, where τ is the pulse duration. The deposited power, $P(r,t)$ per unit length in the target is given as a function of the radial coordinate r by the relation:

$$P(r,t) = \frac{aN_U}{\tau\pi\Delta^2}\,\rho\,\frac{dE}{dz}\,f(t)e^{-ar^2/\Delta^2} \qquad (1)$$

where Δ is the full width at half maximum (FWHM) of the Gaussian ion distribution, N_U is the total number of ions per bunch and dE/dz is the stopping power. The normalizing constant is $a = -4\ln(1/2)$ so that the integral of $P(r,t)$ over the entire beam surface and the pulse duration τ, that is, the energy deposited over a cm-length of uniform target, is $N_U \rho dE/dz$. Using the corresponding stopping power, the total energy deposited per cm by a bunch containing $N_U = 21 \times 0^{11}$ uranium ions is 6.18 kJ and 96 J in a gold target and in a cryogenic hydrogen target, respectively.

A cylindrical gold beam stopper with $r_{off} \geq r_H$ is now designed to shield completely the inner hydrogen sample from the direct heating of the ions. The cylindrical gold beam stopper with radius r_{off} is directly irradiated by the uranium ions and expands laterally. If the gold stopper freely expands in vacuum, the ions loose a fraction of their energy in the expanding plasma entering into the gold absorber with a reduced energy. In this case, the Bragg peak may lie inside the gold absorber, thereby destroying the implosion symmetry. It is therefore necessary to minimize the stopper expansion and at the same time to maintain the transparency of the space just in front of the gold absorber. In order to do that, the two stage target sketched in Figure 1 was designed which shows a cylindrical gold stopper, with radius $r_{off} = r_H + \Delta r$, enclosed within an external aluminum layer which prevent the gold expansion.

After passing through the beam stopper, the incoming ions deposit their energy in the gold absorber. The heated absorber expands and drives the compression of the internal hydrogen sample. In order to have a uniform cylindrical compression of the target, the specific energy deposition along the target axis must be uniform. As known from the Bethe theory (Krane, 1988), the ion energy loss per unit length, the so-called stopping power, is approximately constant only for ions with high kinetic energy, and grows sharply at the end of the ion range producing the Bragg peak. To avoid the non-uniform energy deposition in the Bragg peak region, the target length $L_H + L_S$ must be smaller than the range in the gold absorber.

The stopping power data used in these simulations were obtained employing the numerical code SRIM (Ziegler *et al.*, 1996) and we neglected any effects concerning the ion beam scattering. We assume that a variation up to a few percent in the stopping power along the target length L_H, could be tolerated still providing sufficiently uniform target compression. From SRIM calculations it was found that for a uranium ion in a gold target the stopping power is approximately constant, $(dE/dz)_{Au} = 10^{10}$ eV g/cm^2 within few percents, for ion energy larger than 0.9 GeV/u and with this remaining energy the ion would travel 0.8 cm (almost coinciding with the Bragg peak region) before it is completely stopped.

The stopping power of the uranium ions in hydrogen has also been calculated, the range of a uranium ion of 1 GeV/u in hydrogen is larger than 60 cm (it becomes larger than 2.5 m if the initial energy is 3 GeV/u) and outside the Bragg peak region the stopping power is almost constant and is equal to $(dE/dz)_H = 3.4 \times 10^{10}$ eV g/cm^2.

3. PARAMETIC STUDY

The code MULTI-1D was used to simulate the hydrodynamic evolution of a target irradiated by a uranium ion bunch. The energy deposition of the ions were included in the code taking into account the time and space dependence of the beam, as well as the stopping powers for the gold absorber, $(dE/dz)_{Au} = 10^{10}$ eV g/cm^2, and for the hydrogen sample, $(dE/dz)_H = 3.4\ 10^{10}$ eV g/cm^2. In these simulations SESAME (SESAME, 1992) equation of state has been used.

A set of simulations were performed to evaluate the maximum hydrogen average density, $\rho_M = M_H/(\pi r_s^2 L_H)$, defined as the hydrogen mass divided by its volume evaluated at stagnation time, and the corresponding hydrogen temperature T_M, averaged over the entire hydrogen mass. The collected data are organized in a parametric study in order to show the dependence of ρ_M and T_M with the different beam-target parameters. A series of simulations were performed with ion bunches delivering $N_U = 2 \times 10^{11}$ particles with a Gaussian distribution in space characterized by a FWHM of $\Delta = 1$ mm and $\Delta = 2$ mm . We analyze the performance of targets with a hydrogen radius r_H ranging between 100 to 800 μm. In these cases, the beam stopper has a radius $r_{off} = r_H + \Delta r$, with Δr varying between 0 to 300 μm. This means that we now neglect the energy deposition of the ions in a radius equal to or larger than the radius of the hydrogen sample, see sketch in Figure 1.

The maximum hydrogen compression and the corresponding temperature are computed as a function of r_H and Δr, the shielded gold thickness. The results related to the cases with $\Delta = 1$ mm and $\Delta = 2$ mm are shown in the contour plots in Figures 2 and 3, respectively. Hydrogen temperature is everywhere lower than 0.2 eV with the exception of a small region for $\Delta = 1$ mm, $r_H < 200$ μm and $\Delta r > 200$ μm. As expected, the higher compression factor corresponds to the beam stopper with a radius larger than the hydrogen radius.

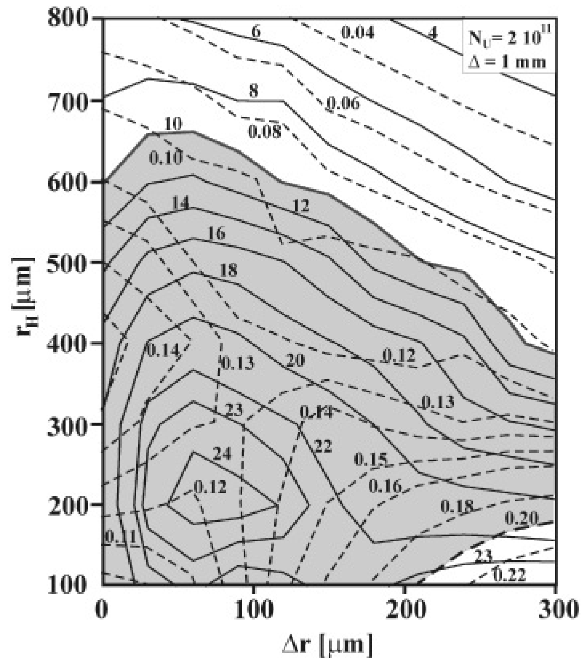

Fig. 2. Contours of the maximum hydrogen compression factor and temperature versus the hydrogen radius, r_H, and the parameter Δr. The shadowed area delimits the window where the compression factor is higher than a factor of 10 and the temperature is smaller than 0.2 eV. The beam delivers $N_U = 2 \times 10^{11}$ particle in a pulse with a Gaussian ion distribution with a $\Delta = 1$ mm.

The shadowed area in Figures 2 and 3, indicates the parametric space where the compression factor is higher than 10, and the hydrogen temperature is lower than 0.2 eV. Both cases show the presence of a maximum in the compression factor, reaching the value of $\rho_M/\rho_H = 24$ for the case of $\Delta =$ 1 mm and $\rho_M/\rho_H = 18$ for $\Delta = 2$ mm. These maximum values are approximately located at about $r_H \approx 200$ μm, $\Delta r \approx 80$ μm for $\Delta = 1$ mm, and $r_H \approx 300$ μm, $\Delta r \approx 100$ μm for $\Delta = 2$ mm. The improved compression of the target with $r_{off} > r_H$ is mainly due to the generation of a cold and heavy pusher between the gold absorber and the internal hydrogen sample (Piriz *et al.*, 2002). The shock moves through the mass of the pusher and then enters the hydrogen. At this time the pusher is moving inward and mainly due to its large inertia it allows for a more efficient compression of the hydrogen sample.

In Figure 3 the target corresponding to $r_H = 300$ μm and $r_{off} = 400$ μm were marked by a star. This point design requires an initial kinetic energy of about 3 GeV/u for target length of $L_H = 2$ cm. This target design is a promising candidate for a future experiment allowing for hydrogen compression at a density higher than 1.6 g/cm^3 (corresponding to a compression factor higher than 18) and a temperature lower than 0.1 eV.

4. 2D SIMULATIONS

The 1D analysis discussed in the previous section indicates that the target design shown in Figure 1 allows for the achieve-

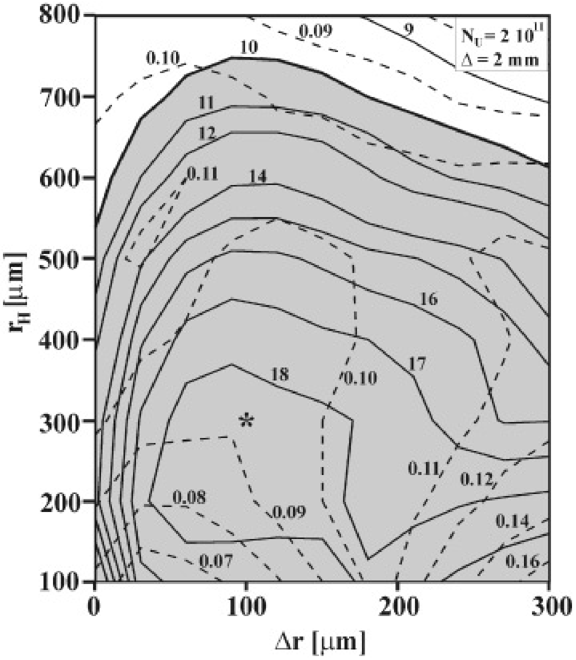

Fig. 3. Same as in Figure 2 but using the Gaussian ion bunch distribution with a FWHM of $\Delta = 2$ mm.

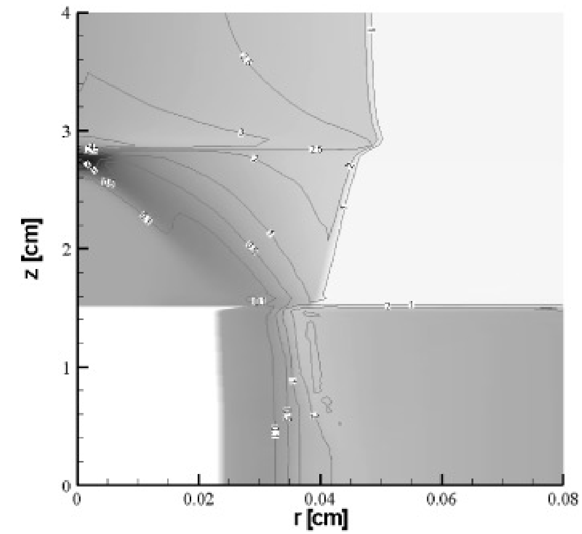

Fig. 4. Two-dimensional density and temperature profile evaluated at time $t = 100$ ns. The simulation refers to the target parameters corresponding to the design point indicated by a star in Figure 3.

ment of high hydrogen densities at relatively low temperature. It was shown that there is a window in the parametric space (r_H, Δ) for which the hydrogen compression factor is higher than 10 and the temperature is lower than 0.2 eV.

2D simulations of the target were done to evaluate the 2D effects that may reduce target performance. The 2D-CAVEAT code was used to perform these simulations. The ion energy deposition was simulated by first splitting the beam into a set of beamlets and their trajectories were tracked. The stopping power is computed along each path taking into account the bound and free electron contributions, and it was used to compute the ion beam energy deposition.

The target is characterized by a hydrogen radius of $r_H = 300\ \mu$m and $r_{off} = 400\ \mu$m corresponding to the point indicated by a star in Figure 3. The ion beam pulse is parabolic in time with $t = 100$ ns and delivers $N_U = 2 \times 10^{11}$ uranium ions. The radial distribution is Gaussian with a FWHM of 2 mm. The density maps evaluated at the end of the ions pulse, $t = 100$ ns and at the stagnation time $t = 181$ ns are shown in Figure 4 and Figure 5, respectively. It is possible to notice the position of the Bragg peak inside the beam stopper that shield the hydrogen target from a direct ion beam irradiation. The large energy deposition associated with the Bragg peak generates a shock moving laterally that compresses the aluminum layer, the gold expansion generate also a shock propagating toward the hydrogen target. The ions crossing the aluminum target reach the gold absorber with energy high enough to still provide a uniform energy deposition along the first 1.5 cm of the gold absorber. Such an energy deposition drives the expansion of the gold absorber that launches a shock through the 100 μm of the payload which moves inward compressing the hydrogen target. It was found that the CAVEAT code provides approximately the same hydrogen target hydrodynamics as found by the 1D MULTI simulations.

It was also found that 2D effects do not significantly change the shape of the compressed hydrogen as shown in Figures 4 and 5. In these frames the isocontours of the electron temperature were added. It is possible to appreciate that at the stagnation, large part of the hydrogen target has a temperature below 0.1 eV.

It is to be noted that hydrogen metallization can be detected in practice by the strong reduction of the electrical resistively produced as a consequence of the super-conducting properties of the metallic hydrogen (Weir *et al.*, 1996). In

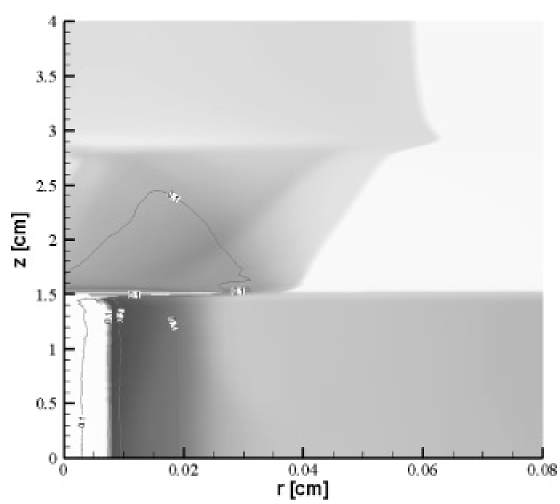

Fig. 5. As in Figure 4 but the density and temperature profile are evaluated at the stagnation time $t = 181$ ns.

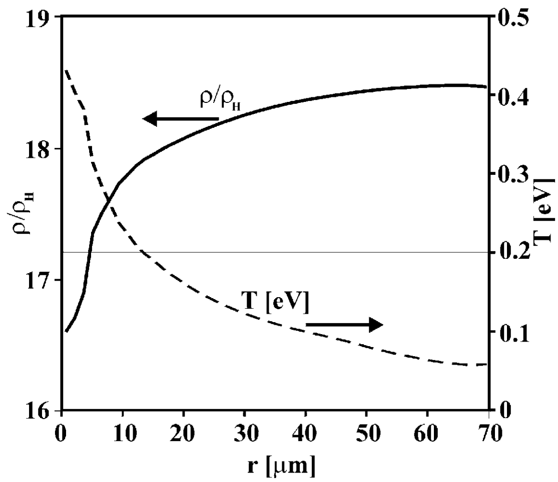

Fig. 6. Hydrogen temperature (T) and compression factor (ρ/ρ_H) as function of the radius r. These profiles are evaluated at stagnation and correspond to the reference case ($N_U = 2 \times 10^{11}$, $\Delta = 2$ mm, $r_H = 300\ \mu$m, $\Delta r = 100\ \mu$m) indicated by a star in Figure 3.

this sense, the spatial profiles of the hydrogen density and temperature may be relevant because the measured electrical current will also depend on the area of the section achieving superconductivity. In Figure 6, we show these profiles evaluated at peak compression for the reference case indicated in Figure 3 by a star. As we can see, the expected metallization conditions (temperature T below 0.2 eV and compression factor ρ/ρ_H above 10) are satisfied for radii larger than approximately 15 μm, so that 96% of the hydrogen has high-conductivity. These profiles are quite typical of all the cases we have studied, and in the worst case, the high-conductivity region is 75% of the total area. Of course this means an uncertainty of 25% in the measured electrical resistively, but actually it should be irrelevant in order to detect metallization as the resistively is expected to be reduced by 3 orders of magnitude (Weir *et al.*, 1996).

5. CONCLUSIONS

The implosion of a two-layer cylindrical target driven by an intense heavy ion bunch was studied. The internal sample is made of cryogenic hydrogen surrounded by a laminar layer made of solid gold. The ion distribution is supposed to have a Gaussian distribution in space and a parabolic profile in time. The pulse length was fixed to $\tau = 100$ ns and the bunch contains a total number of uranium ions, $N_U = 2 \times 10^{11}$. The compression of the hydrogen sample follows from the energy deposition of the uranium ions in the gold absorber. 2D effects like non-uniformity in the energy deposition along the target length and boundary expansion were considered in this study. We also notice that our results may be influenced by the onset of the Rayleigh-Taylor instability at the hydrogen-gold interface during the deceleration phase. However, because of the relatively low value of the acceleration $g \leq 5 \times 10^{12}$ cm/s^2, we expect a number of e-folding lower than 2. Thus, the maximum amplitude of the perturbation remains below a 10% of the final hydrogen radius.

By means of 1D numerical simulations we carried out a parametric study in order to optimize the target design. The study considers hydrogen radius ranging from 100 μm to 800 μm and a total number of ions per bunch $N_U = 2 \times 10^{11}$ with a spatial Gaussian distribution characterized by a FWHM of 1 and 2 mm. Promising results were found considering a target including a beam stopper (with a radius r_{off}) between the incoming ion beam and the hydrogen-gold target. In this way, the hydrogen is not directly heated by the incoming ions, and it can be compressed at very low temperature. Moreover, if $r_{off} > r_H$ the beam stopper generates a cold gold pusher between the absorber and the hydrogen sample providing a more efficient compression.

Average hydrogen compression factors as high as 18 and temperatures lower than 0.1 eV are reached by using $N_U = 2 \times 10^{11}$ uranium ions accelerated to 3 GeV/u and compressed in an bunch having a length $\tau = 100$ ns and a Gaussian spread with $\Delta = 2$ mm driving a target characterized by: hydrogen radius $r_H = 300\ \mu$m, beam stopper radius $r_{off} = 400\ \mu$m, stopper length $L_S = 4.5$ cm and target length L_H of about 2 cm.

2D simulations have been also performed confirming that the 2D effect generated at the boundary of the hydrogen target does not change significantly the cylindrical implosion. The hydrodynamics of the target remain always very close to the 1D results obtained by using MULTI-1D code.

It is expected that this beam-target geometry will allow for producing the phase transition to metallic hydrogen. Since metallic hydrogen is predicted to be a superconductor, such transition can be in principle detected by measuring a strong reduction of the electrical resistively (Weir *et al.*, 1996).

ACKNOWLEDGMENTS

This work was partially supported by the Consejeria de Ciencia y Tecnologia-JCCM-PAI-02-002 (Spain) and by the BMBF (Germany).

REFERENCES

Addessio, F.L., Baumgardner, J.R., Dukowicz, J.K., Johnson, N.L., Kashiwa, B.A., Rauenzahn, R.M. & Zemach, C. (1990). *CAVEAT: A computer code for fluid dynamics problems with large distortion and internal slip* (LA-10613-MS, Rev. 1). Los Alamos, NM: Los Alamos National Laboratory.

Anisimov S.I., Prokhorov A.M. & Fortov V.E. (1984). Application of powerful laser in dynamical physics of high pressure. *Sov. Phys. Usp.* **27** 181–220.

Batani, D., Stabile, H., Ravasio, A., Desai, T., Lucchini, G., Strati, F., Ullschmied, J., Krousky, E., Skala, J., Kralikova, B., Pfeifer, M., Kadlec, C., Mocek, T., Prag, A., Nishimura, H., Ochi, Y., Kilpio, A., Shashkov, E., Stuchebrukhov, I., Vovchenko, V. & Krasuyk, I. (2003). Shock pressure induced by 0.44 μm laser radiation on aluminum targets. *Laser Part. Beams* **21**, 481–487.

Benuzzi, A., Lower, T., Koenig, M., Faral, B., Batani, D., Beretta, D., Danson, C. & Pepler, D. (1996). Indirect and direct laser driven shock waves and applications to copper equation of state measurements in the 10–40 Mbar pressure range. *Phys. Rev. E* **54**, 2162–2165.

Borisenko, N.G., Akunets, A.A., Bushuev, V.S., Dorogotovtsev, V.M. & Merkuliev, Y.A. (2003). Motivation and fabrication methods for inertial confinement fusion and inertial fusion energy targets. *Laser Part. Beams* **21**, 505–509.

Cauble, R., DaSilva, L.B., Perry, T.S., Bach, D.R., Budi, K.S., Celliers, P., Collins, G.W., Ng, A., Barbee, T.W., Hammel, B.A., Holmes, N.C., Kilkenny, J.D., Wallace, R.J., Chiu, G. & Woolsey, N.C. (1997). Absolute measurements of the equations of state of low-Z materials in the multi-Mbar regime using laser-driven shocks. *Phys. Plasmas*, **4**, 1857–1861.

Cauble, R., Phillion, D.W., Hoover, T.J., Holmes, N.C., Kilkenny, J.D. & Lee, R.W. (1993). Demonstration of 0.75 Gbar planar shocks in X-ray driven colliding foils. *Phys. Rev. Lett.* **70**, 2102–2105.

Collins, G.W., Da Silva, L.B., Celliers, P., Gold, D.M., Foord, M.E., Wallace, R.J., Ng, A., Weber, S.V., Budil, K.S. & Cauble, R. (1998). Measurements of the equation of state of deuterium at the fluid insulator-metal transition. *Science* **281**, 1178–1181.

Cottet, F., Romain, J.P., Fabbro, R. & Faral, B. (1984). Ultrahigh pressure laser-driven shock-wave experiments at 0.26 μ-m wavelength. *Phys. Rev. Lett.* **52**, 1884–1886.

Fabbro, R., Faral, B., Virmont, J., Pepin, H., Cottet, F. & Romain, J.P. (1986). Experimental evidence of the generation of multi-hundred megabar pressure in 0.26 μ-m wavelength laser experiments. *Laser Part. Beams* **4**, 413–419.

Godwal, B.K., Rao, R.S., Verma, A.K., Shukla, M., Pant, H.C. & Sikka, S.K. (2003). Equation of state of condensed matter in laser-induced high-pressure regime. *Laser Part. Beams* **21**, 523–528.

Henning, W.F. (2004). The future GSI facility. *Nuclear Instr. Meth. B* **214**, 211–215.

Koenig, M., Faral, B., Boudenne, J. M., Batani, D., Benuzzi, A., Bossi, S., Rémond, C., Perrine, J.P., Temporal, M. & Atzeni, S. (1995). Relative consistency of equations of state by laser-driven shock-waves. *Phys. Rev. Lett.* **74**, 2260–2263.

Krane, K.S. (1988). *Introductory Nuclear Physics*. New York: J. Wiley & Sons.

Lindl, J.D. (1995). Development of the indirect-drive approach to inertial confinement fusion and the target physics basis for ignition and gain. *Phys. Plasmas* **2**, 3933–4024.

More, R.M., Warren, K.H., Young, D.A. & Zimmerman, G.B. (1988). A new quotidian equation of state (QEOS) for hot dense matter. *Phys. Fluids* **31**, 3059–3078.

Nellis, W.J., Mitchell, A.C., McCandless, P.C., Erskine, D.J. & Weir, S.T. (1992). Electronic energy gap of molecular hydrogen from electrical conductivity measurements at high shock pressures. *Phys. Rev. Lett.* **68**, 2937–2940.

Nuckolls, J., Thiessen, A., Wood, L. & Zimmerma, G. (1972). Laser compression of matter to super-high densities-thermonuclear (CTR) applications. *Nature* **239**, 139.

Obenschain, S.P., Whitlock, R.R., McLean, E.A., Ripin, B.H., Price, R.H., Phillion, D.W., Campbell, E.M., Rosen, M.D. & Auerbach, J.M. (1983). Uniform ablative acceleration of targets by laser irradiation at 10^{14} W/cm^2. *Phys. Rev. Lett.* **50**, 44–48.

Piriz, A.R., Portugues, R.F., Tahir, N.A. & Hoffmann, D.H.H. (2002). Analytic model for studying heavy-ion-imploded cylindrical targets. *Laser Part. Beams* **20** 427–429.

Ragan, C.E. (1980). Ultrahigh-pressure shock-wave experiments. *Phys. Rev. A* **21**, 458–463.

Ragan, C.E. (1984). Shock-wave experiments at threefold compression. *Phys. Rev. A* **29**, 1391–1402.

Ragan, C.E., Silbert, M.G. & Diven, B.C. (1977). Shock compression of molybdenum to 2.0 Tpa by means of a nuclear explosion. *J. Appl. Phys.* **48**, 2860–2870.

Ramis, R., Schmalz, R. & Meyer-ter-Vehn, J. (1988). MULTI—A computer code for one-dimensional multigroup radiation hydrodynamics. *Comp. Phys. Com.* **49**, 475–505.

Remington, B.A., Arnett, D., Drake, R.P. & Takabe, H. (1999). Experimental astrophysics—Modeling astrophysical phenomena in the laboratory with intense lasers. *Science* **284**, 1488–1493.

Sesame (1992). The LANL Equation of State Database (Report: LA-UR-92-3407). Springfield, VA: National Technical Information Service.

Tahir, N.A., Hoffmann, D.H.H., Kozyreva, A., Shutov, A., Maruhn, J.A., Neuner, U., Tauschwitz, A., Spiller, A. & Bock, R. (2000). Shock compression of condensed matter using intense beams of energetic heavy ions. *Phys. Rev. E* **61**, 1975–1980.

Tahir, N.A., Hoffmann, D.H.H., Kozyreva, A., Tauschwitz, A., Shutov, A., Maruhn, J.A., Spiller, P., Neuner, U., Jacoby, J., Roth, M., Bock, R., Juranek, H. & Redmer, R. (2001). Metallization of hydrogen using heavy-ion-beam implosion of multilayered cylindrical targets. *Phys. Rev. E* **63**, 016402.

Tahir, N.A., Udrea, S., Deutsch, C., Fortov, V.E., Grandjouan, N., Gryaznov, V., Hoffmann, D.H.H., Hulsmann, P., Kirk, M., Lomonosov, V., Puriz, A.R., Shutov, A., Spiller, P., Temporal., M. & Varentsov, D. (2004). Target heating in high-energy-density matter experiments at the proposed GSI FAIR facility: Non-linear bunch rotation in SIS100 and optimization of spot size and pulse length. *Laser Part. Beams* **22**, 485.

Temporal, M., Piriz, A.R., Grandjouan, N., Tahir, N.A. & Hoffmann, D.H.H. (2003). Numerical analysis of a multilayered cylindrical target compression driven by a rotating intense heavy ion beam. *Laser Part. Beams* **21**, 609–614.

Zeldovich, Y.B. & Raizer, Y.P. (1967). *Physics of shock wave and high temperature hydrodynamic phenomena*. New York: Academic Press.

Ziegler, J.F., Biersack, J.P. & Littmark, U. (1996). *The stopping and ranges of ions in solid*. New York: Pergamon.

Wigner, E. & Huntington, H.B. (1935). The possibility of a metallic modification of hydrogen. *J. Chem. Phys.* **3**, 764–770.

Weir, S.T., Mitchell, A.C. & Nellis, W.J. (1996). Metallization of fluid molecular hydrogen at 140 GPa (1.4 Mbar). *Phys. Rev. Lett.* **76**, 1860–1863.